

Recent Applications of Mesoscale Modeling to Nanotechnology and Drug Delivery

Amitesh Maiti¹, James Wescott³, Paul Kung² and Gerhard Goldbeck-Wood³

¹Chemistry & Materials Science, Lawrence Livermore National Lab, CA 94550, USA

²Accelrys Inc., 10188 Telesis Court, Suite 100, San Diego, CA 92121, USA

³Accelrys Inc., 334 Cambridge Science Park, Cambridge CB4 0WN, UK

ABSTRACT

Mesoscale simulations have traditionally been used to investigate structural morphology of polymer in solution, melts and blends. Recently we have been pushing such modeling methods to important areas of Nanotechnology and Drug delivery that are well out of reach of classical molecular dynamics. This paper summarizes our efforts in three important emerging areas: (1) polymer-nanotube composites; (2) drug diffusivity through cell membranes; and (3) solvent exchange in nanoporous membranes. The first two applications are based on a bead-spring-based approach as encoded in the Dissipative Particle Dynamics (DPD) module. The last application used density-based Mesoscale modeling as implemented in the Mesodyn module.

Keywords: Mesoscale modeling, membranes, diffusion, solvent-exchange.

1 INTRODUCTION

Many interesting problems in soft matter, such as polymer adsorption, polymer-surfactant interaction, microphase separation of block copolymers, formation and coalescence of droplets in emulsion, transport through living cells, and so on can involve spatial inhomogeneities over length-scales ranging between a few nm to a few μm , and exhibit dynamical phenomena over time-scales of 1 ms or greater. Problems at such length and time-scales cannot be directly addressed by either conventional molecular dynamics based on inter-atomic potentials or force fields, or by finite-elements based continuum mechanics. Rather, one needs to take recourse to computational techniques at the intermediate scale, called the mesoscale.

Over the last few years several different approaches have been developed to address problems at the mesoscale. Accelrys' Materials StudioTM suite of software incorporates two distinct methods - a particle-based method called Dissipative Particle Dynamics (DPD) [[1], [2]], and a density-based method called Mesodyn [[3]-[5]]. Traditionally, both these methods have been used to predict morphology of polymers and block copolymers in solutions, melts, and blends, and how they change under the influence of surfactants, temperature, and shear. The

present paper summarizes our efforts to extend such codes to new application areas: (1) studying miscibility and phase-separation in polymer-nanotube composites (DPD); (2) estimating drug diffusivity through cell membranes (DPD); and (3) investigating solvent-exchange phenomena in nanoporous membranes (Mesodyn).

2 POLYMER-NANOTUBE COMPOSITES

The fact that the inclusion of even small amounts of nanomaterial coupled with appropriate processing steps appears to significantly improve mechanical, elastic, thermal, electrical, and optical absorption properties have catapulted nanocomposites to being one of the first practical application areas of nanotechnology. One specific class of composite materials has recently received a lot of attention, i.e., in which carbon nanotubes (CNTs) are dispersed within polymeric matrices [[6], [7]]. Potential applications can range from structural materials, to electromagnetic and heat shielding, to optoelectronics. The physical properties of CNT-polymer composite material depend on the uniformity of CNT dispersion and the degree of parallel alignment within the polymeric matrix, as well as the efficacy of interfacial bonding between the two systems. Since it is difficult to control many of these properties experimentally, modeling and simulations could provide crucial insight and design guidance.

The smallest size and time-scale to describe the morphology of CNT-polymer nanocomposites and its dynamical evolution is currently beyond the capability of standard classical forcefield simulations. We circumvent the problem by coarse-graining both the polymer and the CNT into strings of beads, connected by Hookean springs, and using DPD to hydrodynamically equilibrate such coarse-grained morphology. In DPD [[1], [2]] one represents an entire functional group by a single bead, thereby substantially reducing the number of particles to be simulated. The positions and velocities of the spherical beads are propagated by standard integrators as in regular MD methods and thermally equilibrated through a Langevin thermostat. But rather than interact through Lennard-Jones forces, the beads feel a simple soft pair-wise conservative repulsive potential, which embodies the essential chemistry of the system, and determines whether or not the CNTs disperse in a given polymer. This force is short range and has a simple analytic form resulting in fast computation per time-step. More importantly it provides an

effective time-step of several picoseconds, 3-4 orders of magnitude larger than typical time-steps employed in a MD simulation.

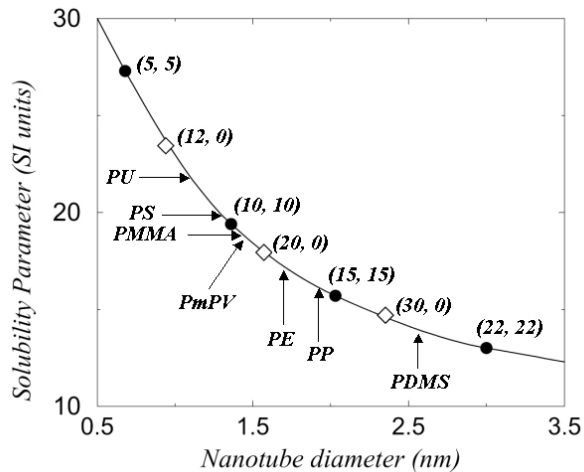


Figure 1. Computed solubility parameter versus tube diameter for armchair (filled circles) and zigzag (unfilled diamonds) CNTs. SYNTHIA-computed solubility values for various polymers are also indicated on the plot for comparison.

The chemistry of polymer-nanotube interaction is incorporated through relating the DPD bead-bead repulsion to the Flory-Huggins χ -parameter [[8]], which in turn is obtained by squaring the difference of pure-component solubility parameters (δ) [[9]]. The latter is defined as the square root of the cohesive energy density. Reliable average values of δ for long-chain polymers can be estimated from simple correlation methods [[10]]. On the other hand, CNTs are not polymers in the conventional sense. Nevertheless, since CNTs tend to form close-packed bundles, a good measure of their cohesive energy can be obtained from the energy cost of isolating a CNT from a bundle. Computing such energy with the Universal Forcefield [[11]] results in δ that is essentially independent of the CNT chiral angle, and that decreases as inverse square-root of the CNT diameter, as illustrated in Fig. 1. Flory-Huggins theory predicts that components with close enough δ , which leads to small DPD repulsion, should mix, while components with significantly differing δ should segregate. Thus, it follows from Fig. 1 that PMMA polymers should mix well with CNTs of diameters close to 1.4 nm (e.g. (10, 10) CNTs), while PP is expected to form uniform composites with CNTs of diameters in the neighborhood of 1.9 nm (e.g. (15, 15) CNTs). The CNT solubility parameter values in Fig. 1 are in great agreement with the experimental result that PmPV polymers mix with CNTs belonging to a narrow diameter range between 1.35-1.55 nm [[12]].

In addition, in order to represent the bending rigidity inherent to carbon nanotubes, we added an angle dependent potential among consecutive triplet of CNT beads:

$$E_{ijk} = \frac{1}{2}k^\theta(1 + \cos\theta_{ijk}).$$

In our DPD simulations each bead (CNT or polymer) was chosen to represent the equilibrium volume of a PMMA monomer (180 \AA^3), implying approximately 12 nm length of the simulated CNTs. Fig. 2 illustrates some of the most interesting results for CNT-PMMA composites with 5% volume fraction of CNTs. These represent typical equilibrium structures after a simulation of 5×10^5 steps, corresponding to a real time of $\sim 9 \mu\text{s}$. As expected, the (10, 10) CNTs readily mix with PMMA (fig. 1(A)), while the (15, 15) (as well as (5, 5) and (9, 0)) segregate (Fig. 1(B)). Fig. 1(C) displays the morphology of dispersed (10, 10) tubes following application of moderate external shear, and opens up the possibility of parallel alignment of the CNTs under realistic shear. For CNTs that don't readily disperse (e.g., the (15, 15)) attachment of appropriate organic functional groups is likely to make them more compatible with the polymer. Fig. 1(D) shows the morphology under such a structural modification, with acrylate monomers attached at regular intervals along the nanotube.

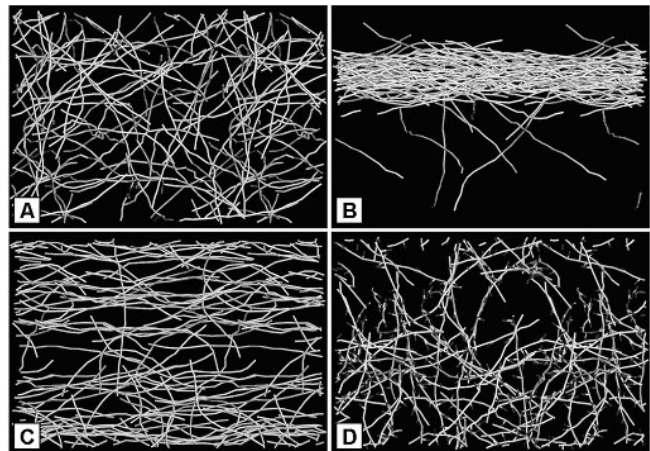


Figure 2. Equilibrium morphologies of CNT-PMMA composites at ambient temperature and pressure as modeled by DPD. CNTs are shown in white, while the PMMA chains are hidden for clarity. (A) Dispersed (10, 10) CNTs; (B) segregated (15,15) CNTs; (C) parallel alignment of (10, 10) CNTs following a shear; (D) dispersion of (15, 15) CNTs functionalized with acrylate groups.

It would be interesting to vary the CNT and polymer lengths, relative compositions, shear rates, and the attached functional groups and investigate the resultant morphology of the nanocomposite. Such morphologies could be represented on a numerical grid, which could then be input to finite-elements-based codes [[13]] in order to compute useful physical properties of the composite. We are also currently investigating other effects, e.g., the efficacy of appropriate triblock copolymers in dispersing CNTs in various solvents, and the effect of reduced dimensionality on CNT dispersion and bundling.

3 DPD MODELING OF DRUG DIFFUSION ACROSS CELL MEMBRANE

The effectiveness of a membrane in allowing the diffusion of a molecule is embodied in a quantity called the Permeability (P), which is defined by the equation $J = -P \Delta c$. Here J is the net number of molecules passing through unit area of the membrane per unit time, Δc is the difference in the concentration of the molecule on either side of the membrane, and the negative sign indicates that the net flow of molecules occurs against the concentration gradient. It can be shown that P is given by:

$$P = \beta D_m / \Delta x,$$

where β is the membrane:water partition coefficient of the molecule (often taken to be the octanol:water partition coefficient), Δx is the membrane width, and D_m the diffusion constant of the molecule through the membrane. While β can be estimated from various solvation schemes within Quantum chemistry codes, the diffusion constant D_m requires dynamical simulations of sufficient time in order to allow the diffusing molecule to move through a distance of at least a few times the average inter-particle spacing. For small molecules like methanol this could be achieved with a classical molecular dynamics simulation of ~ 1 ns, but for larger molecules a much longer simulation becomes necessary. In this section, we discuss our initial exploration into using a mesoscale code like DPD to compute the diffusion constant of small non-electrolyte molecules through a realistic membrane.

The first step is to build a good mesoscale model of the membrane and the diffusing molecule. One could follow the work of Groot and Rabone [[14]] to achieve such a construction, as described in our previous work [[15]]. With such a “meso” setup, it is tempting to run a DPD dynamics simulation and compute the diffusion constant of the drug through the bilayer. Through several initial runs we have verified that molecules like Aspirin can cross the lipid bilayer within just a few hours of CPU time even on a single-processor 600 MHz Pentium PC, while atomistic molecular dynamics do not display significant diffusion even over runs of 1 ns, which can take several days of simulation time. However, the DPD methodology comes with its own set of approximations, especially involving the coarse graining of space and time. So, extracting a physical value of D_m requires careful interpretation and good statistical averaging. Such an effort is currently underway. In the rest of this section, we discuss some observations and thoughts from our explorations so far.

1. Length- and time-scales: The DPD code yields diffusion constant in reduced (*i.e.* dimensionless) units. In order to convert this to a physical unit one needs to calibrate the length-scale and time-scale of the simulation. The length-scale is given by the interaction cutoff

$R_c = (\bar{\rho} V_b)^{1/3}$, where $\bar{\rho}$ is the average DPD bead density in reduced units (typical value being between 3 and 5) and V_b is the bead volume in real physical units. For a molecule that is N_m times the volume of a water molecule ($V_w \approx 30 \text{ \AA}^3$) $R_c = (\bar{\rho} N_m V_w)^{1/3}$. Thus for instance, if $\bar{\rho} = 3$ and $N_m = 3$, one obtains $R_c \approx 6.46 \text{ \AA}$. On the other hand, the time-scale is obtained by performing DPD simulation on liquid water followed by equating the computed self-diffusion constant to the experimental value at room temperature. For $N_m = 1$ and dissipation parameter $\gamma = 4.5$ (in reduced units, see ref. [[1]] for the definition of γ) this yields a time-scale $\tau = 25.7 \text{ ps}$ [[16]]. Scaling of τ with bead-size N_m is discussed below in point 3.

2. Dependence of D_m on the solubility parameter of diffusing molecule: The relative hydrophobicity of the diffusing molecule with respect to the membrane core, which is governed by the difference in their solubility parameters (δ) is reflected in the Flory-Huggin’s χ -parameter, and therefore in the conservative repulsion term in DPD $\Delta \bar{a}$ [[9]]. From preliminary simulations it appears that the diffusion constant of a 1-bead molecule through an amorphous polymer is not very sensitive to $\Delta \bar{a}$ up to moderate values, and then drops sharply for higher $\Delta \bar{a}$. This implies that hydrophilic molecules should take longer to diffuse through the cell membrane than hydrophobic molecules of the same size. However, the simulated D_m also appear to have a strong dependence on the dissipation parameter γ . More simulations at different values of γ and $\Delta \bar{a}$, as well as sophisticated theoretical analysis [[17]] is necessary to see if a quantitatively accurate γ -independent solubility-parameter-dependence can be extracted from DPD simulations.

3. Dependence of D_m on the size of diffusing molecule: Size-dependence of D_m could be directly studied in DPD simulations by representing a bigger bead as a complex of smaller beads connected by springs. Initial simulations suggest that for moderately hydrophobic molecules (solubility parameter $\delta < 30$) D_m is roughly inversely proportional to the bead-size, a feature typical of Rouse-like models in polymer dynamics [[18]]. Results for D_m also appear to be relatively insensitive to the value of polymer spring constant as long as one uses a value 4.0 or greater (in reduced DPD units). Such result, combined with the relative insensitivity of D_m to the solubility parameter of the molecule for moderately hydrophobic drugs (see point 2 above) is consistent with the scaling law $\tau \propto N_m^{5/3}$ as proposed by Groot and Rabone [[14]]. Experimentally, D_m displays a variety of scaling behavior with molecule size, with exponents typically ranging from -0.6 to -1.2 [[19]]. For moderately hydrophobic molecules, our simulated exponent (-1.0) falls somewhere in the middle of the above experimental range.

4. PRECIPITATION MEMBRANE MORPHOLOGY – INVESTIGATION WITH MESODYN

The first two applications involved coarse-graining a group of atoms or functional groups into “beads”, as implemented in the DPD code. In both these applications the fraction of different components remains constant during the simulation. That condition gets violated in this last application, which involves changes in morphology in a polymer membrane when solvent molecules are gradually replaced by non-solvent molecules.

Polymer membranes are widely used in industry for processes such as filtration, dialysis and separation [[20]]. Controlling the morphology of the membrane is of great importance in tailoring them to perform appropriately for specific applications, since it is the size and distribution of pores that largely determines their function. An efficient technique for generating different membrane morphologies is the so-called immersion precipitation, in which a thin film of polymer-solution (resting on a support) is lowered into a bath of non-solvent. After immersion, the solvent diffuses out of the film to be replaced by the non-solvent, which drives precipitation of the polymer. At a certain concentration of non-solvent in the system - the so-called precipitation point - the polymer system is changed from a sol to gel.

To simulate such a phenomenon we employ a density-based mesoscale method called MesoDyn. The algorithm dynamically evolves component density fields defined at discrete grid points, driven by both chemical potential gradients and by Langevin noise towards the free energy minimum. In particular, for the present application we utilize a specific feature of MesoDyn that allows the concentration of the species in a model to be varied. This allows us to gradually exchange the solvent for a non-solvent component. A few details of the algorithm are sketched below.

MesoDyn is based on the Kohn-Sham equivalence scheme between a real system and an ideal (equilibrium) system under a certain external potential. In other words, any system out-of-equilibrium can be regarded as a system in equilibrium but with certain external constraints. The evolution towards equilibrium then becomes an evolution of the external constraints as they reflect the constantly changing state of the system. The component density fields are functionals of the ideal system Hamiltonian (that of Gaussian chains) and a ‘non-ideal’ potential reflecting other interactions.

At the start of a MesoDyn run the density field of a component X is set equal to the average concentration everywhere, i.e. the system is homogeneous. The density fields then evolve according to a stochastic diffusion equation containing the external fields. In fact, MesoDyn solves implicit partial differential equations containing the densities and potentials by means of iterating the potentials

for the next time step until the new density distribution given by the diffusion equation is satisfied. Simulation of solvent exchange requires that the concentration of solvent and non-solvent in the simulation box be changed during the course of the run. Due to the iteration algorithm outlined above, MesoDyn can adapt to changes in concentration, as the solver scheme automatically finds the new potentials which will satisfy the rescaled density fields. Practical variation of concentration was achieved by the development of a perl script to automate the generation of suitable input files, submit the restarted jobs to computational server, and collect the resulting files. This enabled the generation of a single trajectory for the evolution of the system as opposed to a large number of individual frames.

We note, however, that the model in its current form does not take diffusion (nor any glass-transition) into account. In reality the kinetics of non-solvent penetration has a strong controlling effect on the type of morphology produced. Delayed demixing in which the non-solvent is slow to penetrate gives rise to membranes with dense skin layers. The simulation is currently restricted to investigate the instantaneous demixing and the production of bicontinuous phases. Preliminary results from such simulations are published elsewhere [[21]].

ACKNOWLEDGEMENT: We would like to thank Accelrys Inc. for support of this work.

REFERENCES

- [1] R. D. Groot and P. B. Warren, *J. Chem. Phys.* 107, 4423 1997.
- [2] http://www.accelrys.com/mstudio/ms_modeling/dpd.html.
- [3] J.G.E.M. Fraaije, *J. Chem. Phys.* 99, 9202, 1993.
- [4] J.G.E.M. Fraaije et al., *J. Chem. Phys.* 106, 4260, 1997.
- [5] http://www.accelrys.com/mstudio/ms_modeling/mesodyn.html.
- [6] R. H. Baughman et al., *Science* 297, 787, 2002.
- [7] P. M. Ajayan and O. Zhou (2001) in *Carbon Nanotubes Synthesis, Structure, Properties and Applications* (eds. Dresselhaus, M. S.; Dresselhaus, G.; Avouris, P.), Pg. 391-425, Springer-Verlag.
- [8] M. Doi (1996) *Introduction to Polymer Physics*, Chapter 2, Clarendon Press, Oxford.
- [9] A. Maiti, J. Wescott, and P. Kung, *Mol. Sim.* 31, 143, 2005.
- [10] <http://www.accelrys.com/cerius2/synthia.html>.
- [11] A. K. Rappe et al., *J. Am. Chem. Soc.* 114, 10024, 1992.
- [12] A. B. Dalton et al., *J. Phys. Chem. B* 104, 10012, 2000.
- [13] H. R. Lusti and A. A. Gusev, *Modelling. Simul. Mater. Sci. Eng.*, 12, S107, 2004.
- [14] R. D. Groot and K. L. Rabone, *Biophysical Journal* 81, 725, 2001.
- [15] A. Maiti, *NSTI Nanotech* 3, 87, 2004.
- [16] R. D. Groot, *J. Chem. Phys.* 118, 11265, 2003.
- [17] C. Marsh, G. Backx, and M. H. Ernst, M. H., *Europhys. Lett.* 38, 411, 1997.
- [18] M. Doi and S. F. Edwards (1990), “Theory of Polymer Dynamics”, Clarendon, Oxford.
- [19] A. Walter and J. Gutknecht, *J. Membrane Biology* 90, 207, 1986.
- [20] M. H. V. Mulder (1996), “Basic Principles of Membrane Technology”, Kluwer Academic Publishers Group.
- [21] A. Maiti, J. Wescott, and G. Goldbeck-Wood, *Int. J. Nanotech.* (in press, 2005).